Oscillation of the electron-density distribution in momentum space: An $(e, 2e)$ study of H_2 at large momentum transfer

Masakazu Yamazaki,[1] Hironori Satoh,[1] Noboru Watanabe,[1] Darryl B. Jones,[2] and Masahiko Takahashi[1,*]
[1]*Institute of Multidisciplinary Research for Advanced Materials, Tohoku University, Sendai 980-8577, Japan*
[2]*School of Chemical and Physical Sciences, Flinders University, GPO Box 2100, Adelaide SA 5001, Australia*
(Received 29 March 2014; published 12 November 2014)

Bond oscillation, a phenomenon characteristic of the molecular electron-density distribution in momentum space, is demonstrated for the $1\sigma_g$ molecular orbital of H_2 with an $(e, 2e)$ experiment at large momentum transfer. Analysis of the experimental data in terms of two-center interference effects has revealed that different oscillatory structures can be observed, depending on the model for describing $(e, 2e)$ ionization from the constituent H $1s$ atomic orbitals. It is shown that bond oscillation is highly sensitive to the spatial pattern and chemical bonding nature of the molecular orbital.

DOI: 10.1103/PhysRevA.90.052711 PACS number(s): 34.80.Dp

The electronic structure of atoms and molecules can be investigated by electron momentum spectroscopy (EMS), which is $(e, 2e)$ spectroscopy at large momentum transfer [1–3]. It is now well documented that EMS cross sections are directly related to the one-electron momentum density distribution of the ionized molecular orbital (MO). EMS can therefore offer an opportunity to study various properties of MOs in momentum-space (p-space), rather than through the usual position-space (r-space) description [1–3]. Such p-space concepts [4,5] are common in solid-state physics, while they are encountered less frequently in atomic and molecular physics.

In p space, the constituent atomic orbitals (AOs) of a MO are centered at the origin, and the information about the nuclear positions ($\boldsymbol{R}_j$) is only present in phase factors, $\exp(-i\,\boldsymbol{p}\cdot\boldsymbol{R}_j)$, introduced by the Dirac-Fourier transform. Hence the electron momentum density of a MO should exhibit, for example, cosinusoidal or sinusoidal modulation with periodicity of $2\pi/R_{jk}$ along the bonding direction, where R_{jk} is the distance between atoms j and k. These oscillation phenomena, characteristic of molecular electron-density distributions in p space, are called bond oscillation [5,6] and its prediction can be traced back to the early 1940s [4].

Experimental evidence of bond oscillation was, however, given only recently for the three outermost MOs of CF_4, each of which consisted of a combination of nonbonding $2p$ AOs located on the four F atoms [7]. This study showed not only the presence of bond oscillation but also its sensitivity to the spatial orientation of the constituent AOs. These observations can also be recognized as a result of four-center interference effects in EMS cross sections, i.e., coherent $(e, 2e)$ scattering from the four different molecular centers at large momentum transfer. In this regard, bond oscillation may be a phenomenon analogous to the Cohen-Fano oscillations [8] or the Young-type double-slit interference [9] observed by photon- [8,10–12], electron- [13–17] and ion-impact [18,19] studies for diatomic molecules. Note, however, that those studies measured interference patterns in the energy and angular distributions of free electrons emitted from molecules, and not the interference effects (bond oscillations) in the momenta of electrons when they are bound to molecules.

Very recently, Zhang *et al.* [20] have reported a high-energy-resolution (0.6 eV) EMS study on H_2 by using their state-of-the-art spectrometer [21]. Here the observed deviation from the Franck-Condon principle in vibrational ratio was ascribed to two-center interference effects. However, the oscillatory features due to bond oscillation remain somewhat unclear owing to the large statistical uncertainties of the experimental data and the narrow momentum range covered (<1 a.u.). A much wider range of momenta up to $2\pi/R_{\mathrm{HH}} = 4.5$ a.u. is at least required to observe the complete period of bond oscillation in H_2, having the internuclear distance R_{HH} of 1.4 a.u. In fact, it has long been believed that it is unlikely that bond oscillation in H_2 could be experimentally observed, with an additional difficulty caused by the very small amplitude of the expected oscillation [22,23].

In this paper, we report an EMS study on bond oscillation in H_2, while greatly extending the earlier study on CF_4 [7]. This extension is twofold. First, by employing our latest EMS spectrometer [24] a substantially wider momentum range of up to 6 a.u. is covered, compared with that done in the study on CF_4 (<3.6 a.u.). Here particular stress is placed upon achieving high statistical precision at the expense of energy resolution. Second, the influence of chemical bonding on the bond oscillation behavior is investigated. H_2 is the simplest molecule but its $1\sigma_g$ MO forms a covalent bond. This is in sharp contrast to the study on CF_4 [7]. It is shown that bond oscillation is highly sensitive to spatial pattern and the chemical bonding nature of the $1\sigma_g$ MO.

EMS involves coincident detection of the two outgoing electrons produced by electron-impact ionization at large momentum transfer [1–3]. Through the conservation of energy and linear momentum, binding energy of the target electron (E_{bind}) and recoil momentum of the residual ion ($\boldsymbol{q}$) can be determined:

$$E_{\mathrm{bind}} = E_0 - E_1 - E_2, \tag{1}$$

$$\boldsymbol{q} = \boldsymbol{p}_0 - \boldsymbol{p}_1 - \boldsymbol{p}_2. \tag{2}$$

Here E_j's and $\boldsymbol{p}_j$'s ($j = 0,1,2$) are kinetic energies and momenta of the incident, inelastically scattered and ejected electrons, respectively. Since the collision kinematics of EMS

*masahiko@tagen.tohoku.ac.jp

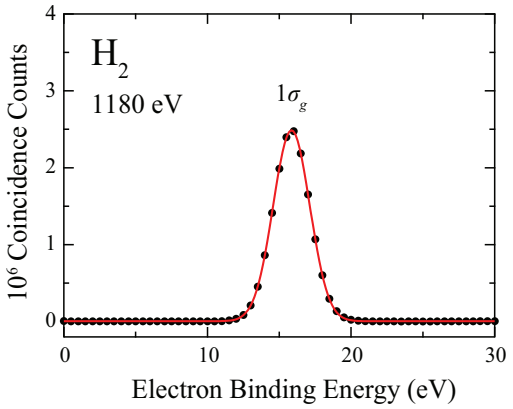

FIG. 1. (Color online) $\Delta\phi$-angle integrated binding energy spectrum of H_2.

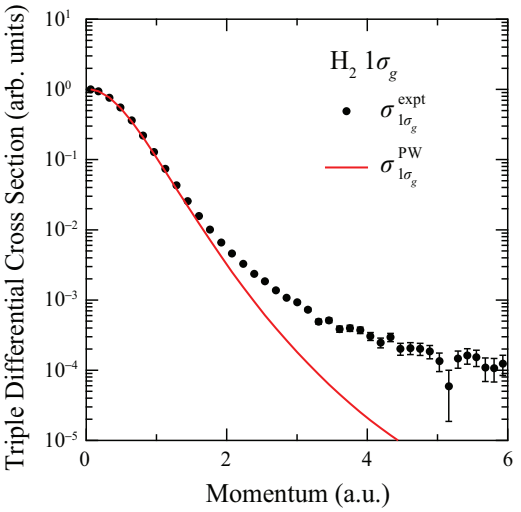

FIG. 2. (Color online) Comparison of experimental and theoretical momentum profiles for the $(1\sigma_g)^{-1}$ ionization transition of H_2.

most nearly corresponds to a collision of two free electrons with the residual ion acting as a spectator, the momentum of the target electron $\boldsymbol{p}$, before ionization, is equal in magnitude and opposite in sign to $\boldsymbol{q}$ ($\boldsymbol{p} = -\boldsymbol{q}$). In the symmetric noncoplanar geometry, two outgoing electrons having equal energies ($E_1 = E_2$) and making equal scattering angles ($\theta_1 = \theta_2 = 45^\circ$) are detected. The magnitude of the target electron momentum p is given by

$$p = \sqrt{(p_0 - \sqrt{2}p_1)^2 + [\sqrt{2}p_1 \sin(\Delta\phi/2)]^2}, \qquad (3)$$

with $\Delta\phi$ being the out-of-plane azimuthal-angle difference between the two outgoing electrons [24].

The EMS experiment on H_2 was conducted at E_0 of 1180 eV, by using our latest spectrometer [24] that covers almost the complete $\Delta\phi$-angle range available for the symmetric noncoplanar $(e, 2e)$ reaction. Briefly, electron-impact ionization occurs where an incident electron beam collides with a gaseous H_2 target. Two outgoing electrons emerging at the scattering angle of 45° are detected with a spherical analyzer followed by a large-area position-sensitive detector (RoentDek Handels GmbH, HEX120). The experimental results for H_2 were obtained by accumulating data for 15 days run time at ambient sample gas pressure of 4.5×10^{-4} Pa. The instrumental energy and momentum resolution employed were 2.7 eV full width at half maximum (FWHM) and 0.26 a.u. at $\Delta\phi = 0^\circ$, respectively.

Figure 1 shows a $\Delta\phi$-angle integrated binding energy spectrum of H_2. It can be seen that although the employed energy resolution does not allow a separation of vibrational levels in the final $(1\sigma_g)^{-1}$ ionic state, the statistical precision of the data is remarkably high. In fact, the number of the true coincidence events accumulated for the $(1\sigma_g)^{-1}$ ionization band amounts to $\sim 1.5 \times 10^7$, which is two to three orders of magnitude larger than $\sim 3.5 \times 10^4$ obtained in the EMS study on H_2 by Zhang *et al.* [20]. A similar counting procedure was repeated for a series of spectra at each $\Delta\phi$ angle to create the momentum profile for the $1\sigma_g$ MO, $\sigma^{\text{expt}}_{1\sigma_g}$, shown in Fig. 2. Here, $\sigma^{\text{expt}}_{1\sigma_g}$ is height normalized so as to have the intensity of unity at $p = 0.06$ a.u. ($\Delta\phi = 0^\circ$). The momentum range covered up to 6 a.u. may be wide enough to investigate the bond oscillation in H_2. However, there are two issues to be considered before undertaking such an investigation. One is the choice of theoretical model to describe bond oscillation in H_2, and the other is the range of momenta over which the plane-wave impulse approximation (PWIA) is valid [1–3].

We begin by first discussing the choice of theoretical model. The $1\sigma_g$ MO of H_2, $\psi_{1\sigma_g}(\boldsymbol{r})$, can be described as a linear combination of $1s$ AOs of two H atoms $\varphi_{1s}(\boldsymbol{r})$:

$$\psi_{1\sigma_g}(\boldsymbol{r}) = [\varphi_{1s}(\boldsymbol{r} - \boldsymbol{R}_1) + \varphi_{1s}(\boldsymbol{r} - \boldsymbol{R}_2)]/(2 + 2S)^{1/2}. \quad (4)$$

Here $\boldsymbol{R}_1$ and $\boldsymbol{R}_2$ are the nuclear positions of the two H atoms and S is the overlap integral. The Dirac-Fourier transform of $\psi_{1\sigma_g}(\boldsymbol{r})$ provides the p-space MO, $\psi_{1\sigma_g}(\boldsymbol{p})$, as

$$\psi_{1\sigma_g}(\boldsymbol{p}) = [\exp(-i\,\boldsymbol{p}\cdot\boldsymbol{R}_1) + \exp(-i\,\boldsymbol{p}\cdot\boldsymbol{R}_2)]\varphi_{1s}(\boldsymbol{p})/(2 + 2S)^{1/2}, \qquad (5)$$

with $\varphi_{1s}(\boldsymbol{p})$ being the p-space representation of $\varphi_{1s}(\boldsymbol{r})$. Then one has the spherically averaged quantity of $|\psi_{1\sigma_g}(\boldsymbol{p})|^2$ or the $1\sigma_g$ electron momentum profile, $F_{1\sigma_g}(p)$ (Refs. [4,22]):

$$F_{1\sigma_g}(p) = (4\pi)^{-1} \int d\Omega |\psi_{1\sigma_g}(\boldsymbol{p})|^2 = F_{1s}(p)[1 + \sin(pR_{\text{HH}})/pR_{\text{HH}}]/(1 + S). \quad (6)$$

Here $F_{1s}(p)$ is the spherically averaged quantity of $|\varphi_{1s}(\boldsymbol{p})|^2$. The function $[1 + \sin(pR_{\text{HH}})/(pR_{\text{HH}})]$ in Eq. (6) brings about modulation into $F_{1\sigma_g}(p)$, so it is henceforth referred to as the interference factor. Note that Eq. (6) has the same form as the Cohen-Fano interference factor [8] but they are distinctly different physical quantities, i.e., momenta of bound and free electrons, respectively, as mentioned earlier.

We now consider the somewhat awkward second issue regarding the range of momenta over which PWIA is valid. Generally speaking, PWIA is the most widely used $(e, 2e)$ scattering model in EMS, which gives the EMS cross section for the $(1\sigma_g)^{-1}$ ionization transition of a gaseous H_2

target, $\sigma_{1\sigma_g}(p)$, as

$$\sigma_{1\sigma_g}(p) = (2\pi)^4 \frac{p_1 p_2}{p_0} f_{ee}(4\pi)^{-1} \int d\Omega \left|\psi_{1\sigma_g}(\boldsymbol{p})\right|^2 = (2\pi)^4 \frac{p_1 p_2}{p_0} f_{ee} F_{1\sigma_g}(p), \quad (7)$$

with f_{ee} being the electron-electron collision factor. It is obvious from Eq. (7) that PWIA directly connects the experimental EMS cross sections to the momentum profile of the ionized orbital. Hence, within PWIA, one can extract in a straightforward fashion the interference factor from the experimental data. For instance, in the case of the $1\sigma_g$ MO of H_2 dividing the experimental $\sigma_{1\sigma_g}(p)$ by a theoretical momentum profile $\sigma_{1s}(p)$ of a constituent AO gives

$$\sigma_{1\sigma_g}(p)/\sigma_{1s}(p) \propto [1 + \sin(pR_{HH})/pR_{HH}]. \quad (8)$$

In this regard, however, one needs to be mindful of the fact that PWIA is usually valid only for momentum values up to ~1.5 a.u. at E_0 values of the order of 1 keV [1–3]. This means that a study on bond oscillation in H_2 should entail compensation for the failure of the PWIA description at larger momenta above ~1.5 a.u. In order to illustrate this situation, a theoretical $1\sigma_g$ momentum profile obtained within PWIA, $\sigma^{PW}_{1\sigma_g}$, is included in Fig. 2. Here the PWIA result was calculated by approximating $\psi_{1\sigma_g}(\boldsymbol{p})$ in Eq. (7) as the p-space representation of a Kohn-Sham (KS) orbital [25], generated by the GAUSSIAN98 program [26] using the B3LYP functional [27] with the d-aug-cc-pVTZ basis set [28]. It was subsequently folded with the instrumental momentum resolution and was also height normalized to compare with the experiment. It is evident from Fig. 2 that while PWIA reproduces well the experiment at small momenta below ~1.5 a.u., at larger momenta PWIA substantially underestimates the experimental intensity. Such a tendency of PWIA has commonly been observed in previous EMS studies on various targets [1–3] and it has been attributed to distorted-wave effects [1,29]. This is because, as the Dirac-Fourier transform indicates, the larger p region of EMS experiments involves contributions from the r-space regions closer to the nuclei, where the potentials of the target and the residual ion may distort the incoming and outgoing electrons from plane waves. The distorted-wave impulse approximation (DWIA) [1,29] is an $(e, 2e)$ scattering model that was designed to include distorted-wave effects for EMS. DWIA gives the EMS cross section for the $(1s)^{-1}$ ionization transition of a H atom, $\sigma^{DW}_{1s}(p)$, as

$$\sigma^{DW}_{1s}(p) = (2\pi)^4 \frac{p_1 p_2}{p_0} f_{ee} \times \sum_{av} |\langle \chi^{(-)}(\boldsymbol{p}_1)\chi^{(-)}(\boldsymbol{p}_2)|\chi^{(+)}(\boldsymbol{p}_0)\varphi_{1s}\rangle|^2. \quad (9)$$

Here, $\sum_{av}$ represents a sum over final- and average over initial-state degeneracies. $\chi^{(+)}(\boldsymbol{p}_0)$ and $\chi^{(-)}(\boldsymbol{p}_1)$ $[\chi^{(-)}(\boldsymbol{p}_2)]$ are the distorted waves representing the incident and outgoing electrons moving in the static potential of the neutral H atom and that of the residual ion H^+, respectively. Although DWIA calculations are not yet available for any molecules due to difficulties in working with the multicentered distorting potential, for atoms DWIA is known to satisfactorily resolve the differences at larger momenta between experiments and PWIA [1–3]. In particular, a recent study on Ne [24] has shown that DWIA is valid over a range of momenta up to 8 a.u.

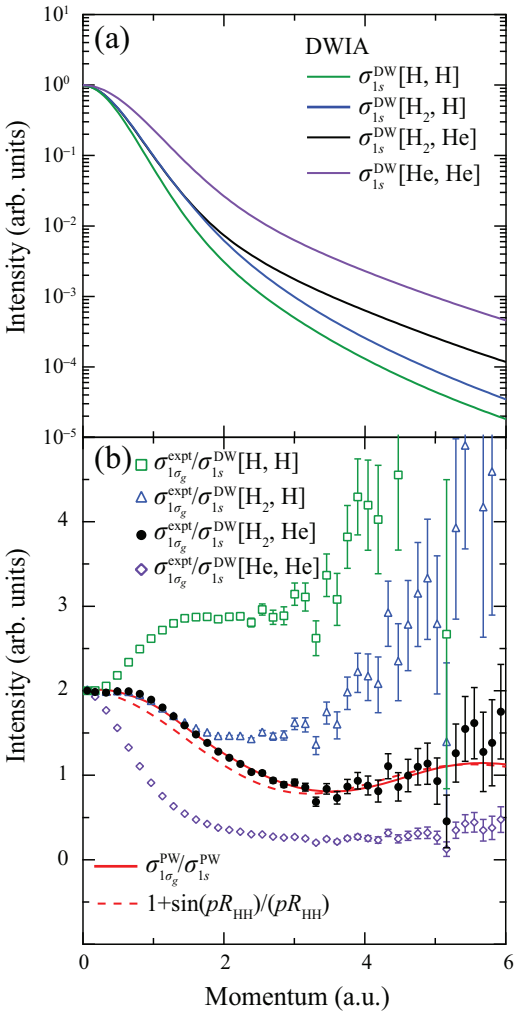

FIG. 3. (Color online) (a) Theoretical momentum profiles for the $(1s)^{-1}$ ionization transition of H and He. (b) Comparison of experimental, theoretical, and analytical interference factors for bond oscillation of H_2. See text for details.

Having addressed the aforementioned two issues, the following data analysis has been made to assess bond oscillation in H_2. Figure 3(a) shows four theoretical momentum profiles employed as $\sigma_{1s}(p)$ in Eq. (8), each of which is height normalized so as to have the intensity of unity at $p = 0.06$ a.u. Here, all four of the calculations were made using the DWIA [30], but with different AOs and/or distorting potentials. σ^{DW}_{1s} [H, H] was calculated using the exact $1s$ AO of H as φ_{1s} in Eq. (9) with the potential for H. σ^{DW}_{1s} [H_2, H] was obtained using the same potential but with a different AO for φ_{1s}. Here, a linear combination function for one H atom was generated by picking all the s-type components out of the $1\sigma_g$ KS MO of H_2. In the procedure, it was found that more than 98% of the norm of the $1\sigma_g$ KS MO is accounted for by the s-type expansion functions. The linear combination function was then employed as φ_{1s} after being renormalized. σ^{DW}_{1s} [H_2, He] was calculated with the same φ_{1s} used for σ^{DW}_{1s} [H_2, H], but with the potential for He. σ^{DW}_{1s} [He, He] was calculated as a reference by using

the Hartree-Fock $1s$ orbital of He and the potential for He. The resulting experimental interference factors are presented in Fig. 3(b). They were obtained by dividing $\sigma_{1\sigma_g}^{\rm expt}$ in Fig. 2 by the corresponding theoretical momentum profile in Fig. 3(a) and by performing a normalization so that they all have the value of 2 at $p = 0.06$ a.u. As another reference, a theoretical interference factor $\sigma_{1\sigma_g}^{\rm PW}/\sigma_{1s}^{\rm PW}$ as well as the analytical factor $[1 + \sin(pR_{\rm HH})/(pR_{\rm HH})]$ is included in Fig. 3(b). $\sigma_{1\sigma_g}^{\rm PW}/\sigma_{1s}^{\rm PW}$ was calculated by dividing $\sigma_{1\sigma_g}^{\rm PW}$ in Fig. 2 by the PWIA momentum profile of the linear combination function.

It is evident from Fig. 3(b) that the four experimental interference factors show different oscillatory structures, depending upon the model for $\sigma_{1s}(p)$. $\sigma_{1\sigma_g}^{\rm expt}/\sigma_{1s}^{\rm DW}$ [H, H] exhibits significant deviations, in terms of both phase and amplitude, from $[1 + \sin(pR_{\rm HH})/(pR_{\rm HH})]$. Note that the phase of $\sigma_{1\sigma_g}^{\rm expt}/\sigma_{1s}^{\rm DW}$ [H, H] indicates an unacceptable orbital spatial pattern as if the $1\sigma_g$ MO were antibonding resulting from destructive interference between the two $1s$ AOs. $\sigma_{1\sigma_g}^{\rm expt}/\sigma_{1s}^{\rm DW}$ [H_2, H] considerably reduces the deviations; a good agreement with $[1 + \sin(pR_{\rm HH})/(pR_{\rm HH})]$ can be seen in a limited momentum range up to $\sim$1.5 a.u. This observation can be understood by switching one's eyes to Fig. 3(a) where with the increase in momentum the intensity of $\sigma_{1s}^{\rm DW}$ [H_2, H] falls off more slowly than that of $\sigma_{1s}^{\rm DW}$ [H, H]. By keeping in mind the nature of the Dirac-Fourier transform that high electron density in the r-space regions close to the nuclei leads to high density at large p and vice versa, the observation in Fig. 3(b) therefore confirms the well-known knowledge that the $1s$ AOs of two isolated H atoms shrink upon formation of the H_2 molecule. Indeed, the linear combination function indicates that the most probable distance between the proton and electron is 0.81 a.u., smaller than the Bohr radius of an isolated H atom. Furthermore, a good agreement over the entire momentum range can be obtained by $\sigma_{1\sigma_g}^{\rm expt}/\sigma_{1s}^{\rm DW}$ [H_2, He]. This observation might be able to be understood from the fact that H_2 is a two-electron system. In the real H_2 distorting potential case, the residual H_2^+ ion still has one $1\sigma_g$ electron and hence the effective nuclear charge is changeable. For instance, when the binary electron-electron collision takes place in the internuclear, chemical bonding region, the net effective nuclear charge for the two outgoing electrons is likely to be larger than the fixed value of $+1$ in the H potential case, as the remaining $1\sigma_g$ electron has the greatest probability of existing outside or at the "reduced" Bohr radius (0.81 a.u.) with less shielding of the nuclear charge. These situations in H_2 can be simulated with the isoelectronic system He ($\sigma_{1s}^{\rm DW}$ [H_2, He]) but not with H ($\sigma_{1s}^{\rm DW}$ [H_2, H]). A similar argument is also possible for distortion of the incoming electron. However, this understanding is merely a speculation, so the observation eagerly awaits detailed theoretical explanations.

The above-mentioned observations superficially appear to be a high-energy confirmation of the findings by Milne-Brownlie *et al.* [14] and by Casagrande *et al.* [15]. For example, in the latter study [15] the ejected-electron angular distribution in the coplanar asymmetric $(e, 2e)$ cross sections of H_2 at E_0 values of several hundreds of eV was found to agree nicely with the Cohen-Fano interference factor when the denominator was experimental $(e, 2e)$ cross sections for He. However, such cases are different with bond oscillation in H_2. It is clear from Fig. 3(b) that $\sigma_{1\sigma_g}^{\rm expt}/\sigma_{1s}^{\rm DW}$ [He, He] is vastly different from $[1 + \sin(pR_{\rm HH})/(pR_{\rm HH})]$. This demonstrates the unique ability of EMS to measure momenta and energies of electrons bound in matter.

Finally, it may be worthwhile to note that in Fig. 3(b) there is a small but noticeable discrepancy between $\sigma_{1\sigma_g}^{\rm expt}/\sigma_{1s}^{\rm DW}$ [H_2, He] and $[1 + \sin(pR_{\rm HH})/(pR_{\rm HH})]$. The agreement of $\sigma_{1\sigma_g}^{\rm expt}/\sigma_{1s}^{\rm DW}$ [H_2, He] with $\sigma_{1\sigma_g}^{\rm PW}/\sigma_{1s}^{\rm PW}$ is surprisingly good and thereby we believe that the discrepancy is real. A possible clue for understanding the discrepancy may be to consider the missing components in constructing the linear combination function; p-type and d-type components. Thus analysis of the discrepancy is expected to give a deeper insight into chemical bonding effects beyond the s-type shrinkage framework examined here. However, we leave such discussion, regarding angular deformation of AOs upon molecular formation, for future high-statistics experiments with a wider range of momenta. Furthermore, we expect that the inherent ability of bond oscillation to simultaneously investigate the molecular structure and electronic wave function can be cultivated for various targets.

This work was partially supported by Grant-in-Aids for Scientific Research (S) (No. 20225001) and for Young Scientists (B) (No. 21750005) from the Ministry of Education, Culture, Sports, Science and Technology. D.B.J. acknowledges financial support from an Australian Research Council DECRA.

[1] E. Weigold and I. E. McCarthy, *Electron Momentum Spectroscopy* (Kluwer Academic/Plenum, New York, 1999), and references therein.

[2] M. A. Coplan, J. H. Moore, and J. P. Doering, Rev. Mod. Phys. **66**, 985 (1994).

[3] M. Takahashi, Bull. Chem. Soc. Jpn. **82**, 751 (2009).

[4] For example, C. A. Coulson, Proc. Cambridge Philos. Soc. **37**, 55 (1941); C. A. Coulson and W. E. Duncanson, *ibid.* **37**, 67 (1941).

[5] I. R. Epstein and A. C. Tanner, in *Compton Scattering*, edited by B. G. Williams (McGraw-Hill, New York, 1977).

[6] J. P. D. Cook and C. E. Brion, Chem. Phys. **69**, 339 (1982).

[7] N. Watanabe, X.-J. Chen, and M. Takahashi, Phys. Rev. Lett. **108**, 173201 (2012).

[8] H. D. Cohen and U. Fano, Phys. Rev. **150**, 30 (1966).

[9] M. F. Ciappina, O. A. Fojón, and R. D. Rivarola, J. Phys. B **47**, 042001 (2014).

[10] M. Walter and J. Briggs, J. Phys. B **32**, 2487 (1999).

[11] D. Akoury, K. Kreidi, T. Jahnke, Th. Weber, A. Staudte, M. Schöffler, N. Neumann, J. Titze, L. Ph. H. Schmidt, A. Czasch, O. Jagutzki, R. A. Costa Fraga, R. E. Grisenti, R. Díez Muiño,

N. A. Cherepkov, S. K. Semenov, P. Ranitovic, C. L. Cocke, T. Osipov, H. Adaniya *et al.*, Science **318**, 949 (2007).
[12] S. E. Canton, E. Plésiat, J. D. Bozek, B. S. Rude, P. Decleva, and F. Martín, Proc. Natl. Acad. Sci. USA **108**, 7302 (2011).
[13] C. R. Stia, O. A. Fojón, P. F. Weck, J. Hanssen, and R. D. Rivarola, J. Phys. B **36**, L257 (2003).
[14] D. S. Milne-Brownlie, M. Foster, J. Gao, B. Lohmann, and D. H. Madison, Phys. Rev. Lett. **96**, 233201 (2006).
[15] E. M. Staicu Casagrande, A. Naja, F. Mezdari, A. Lahmam-Bennani, P. Bolognesi, B. Joulakian, O. Chuluunbaatar, O. Al-Hagan, D. H. Madison, D. V. Fursa, and I. Bray, J. Phys. B **41**, 025204 (2008).
[16] S. Chatterjee, S. Kasthurirangan, A. H. Kelkar, C. R. Stia, O. A. Fojón, R. D. Rivarola, and L. C. Tribedi, J. Phys. B **42**, 065201 (2009).
[17] Z. N. Ozer, H. Chaluvadi, M. Ulu, M. Dogan, B. Aktas, and D. Madison, Phys. Rev. A **87**, 042704 (2013).
[18] N. Stolterfoht, B. Sulik, V. Hoffmann, B. Skogvall, J. Y. Chesnel, J. Rangama, F. Frémont, D. Hennecart, A. Cassimi, X. Husson, A. L. Landers, J. A. Tanis, M. E. Galassi, and R. D. Rivarola, Phys. Rev. Lett. **87**, 023201 (2001).
[19] D. Misra, U. Kadhane, Y. P. Singh, L. C. Tribedi, P. D. Fainstein, and P. Richard, Phys. Rev. Lett. **92**, 153201 (2004).
[20] Z. Zhang, X. Shan, T. Wang, E. Wang, and X. Chen, Phys. Rev. Lett. **112**, 023204 (2014).
[21] X. Shan, X. J. Chen, L. X. Zhou, Z. J. Li, T. Liu, X. X. Xue, and K. Z. Xu, J. Chem. Phys. **125**, 154307 (2006).
[22] E. Weigold, Aust. J. Phys. **35**, 571 (1982).
[23] K. T. Leung and C. E. Brion, Chem. Phys. **82**, 113 (1983).
[24] M. Yamazaki, H. Satoh, M. Ueda, D. B. Jones, Y. Asano, N. Watanabe, A. Czasch, O. Jagutzki, and M. Takahashi, Meas. Sci. Technol. **22**, 075602 (2011).
[25] P. Duffy, D. P. Chong, M. E. Casida, and D. R. Salahub, Phys. Rev. A **50**, 4707 (1994).
[26] M. J. Frisch *et al.*, *GAUSSIAN98, Revision A.7* (Gaussian, Inc., Pittsburgh PA, 1998).
[27] A. D. Becke, J. Chem. Phys. **98**, 5648 (1993).
[28] T. H. Dunning, Jr., J. Chem. Phys. **90**, 1007 (1989).
[29] I. E. McCarthy and E. Weigold, Phys. Rep. **27**, 275 (1976).
[30] I. E. McCarthy, Aust. J. Phys. **48**, 1 (1995).